# Curvature effects on lipid packing and dynamics in liposomes revealed by coarse grained molecular dynamics simulations

Risselada, H. Jelger; Marrink, Siewert J.

*Published in:*
Physical Chemistry Chemical Physics

*DOI:*
10.1039/b818782g



*Publication date:*
2009

# Curvature effects on lipid packing and dynamics in liposomes revealed by coarse grained molecular dynamics simulations

**H. Jelger Risselada and Siewert J. Marrink***

*Received 22nd October 2008, Accepted 16th January 2009*
*First published as an Advance Article on the web 29th January 2009*
**DOI: 10.1039/b818782g**

The molecular packing details of lipids in planar bilayers are well characterized. For curved bilayers, however, little data is available. In this paper we study the effect of temperature and membrane composition on the structural and dynamical properties of a liposomal membrane in the limit of high curvature (liposomal diameter of 15–20 nm), using coarse grained molecular dynamics simulations. Both pure dipalmitoyl phosphatidylcholine (DPPC) liposomes and binary mixtures of DPPC and either dipalmitoylphosphatidylethanolamine (DPPE) or polyunsaturated dilinoleylphosphatidylcholine (DLiPC) lipids are modeled. We take special care in the equilibration of the liposomes requiring lipid flip-flopping, which can be facilitated by the temporary insertion of artificial pores. The equilibrated liposomes show some remarkable properties. Curvature induces membrane thinning and reduces the thermal expansivity of the membrane. In the inner monolayer the lipid head groups are very closely packed and dehydrated, and the lipids tails relatively disordered. The opposite packing effects are seen in the outer monolayer. In addition, we noticed an increased tendency of the lipid tails to backfold toward the interface in the outer monolayer. The distribution of lipids over the monolayers was found to be strongly temperature dependent. Higher temperatures favor more equally populated monolayers. Relaxation times of the lipid tails were found to increase with increasing curvature, with the lipid tails in the outer monolayer showing a significant slower dynamics compared to the lipid tails in the inner monolayer. In the binary systems there is a clear tendency toward partial transversal demixing of the two components, with especially DPPE enriched in the inner monolayer. This observation is in line with a static shape concept which dictates that inverted-cone shaped lipids such as DPPE and DLiPC would prefer the concave volume of the inner monolayer. However, our results for DLiPC show that another effect comes into play that is almost equally strong and provides a counter-acting driving force toward the outer, rather than the inner monolayer. This effect is the ability of the polyunsaturated tails of DLiPC to backfold, which is advantageous in the outer monolayer. We speculate that polyunsaturated lipids in biological membranes may play an important role in stabilizing both positive and negative regions of curvature.

## 1. Introduction

Liposomes, or vesicles, are widely used in *in vitro* studies as mimics of either complete cells or cell organelles such as endosomes or transport vesicles involved in endo- or exocytosis and protein trafficking. In the realm of synthetic biology they furthermore play an important role as drug carriers, sensors and many more potential applications only limited by imagination. Below a certain critical length scale the physical properties of the liposomal membrane becomes dependent on its radius. For instance, small liposomes possess a high bending energy, which affects their fusogenic propensity. The smaller the radius of a liposome, the more likely and faster it will fuse. Not surprisingly, in nature fusion processes are mediated by small vesicles. Experimentally the smallest liposomes that can be formed by sonication are in the order of 20 nm.[1] It is plausible that these vesicles are in fact metastable, and will fuse to form larger vesicles if they get the chance. Another illustration of altered properties of curved bilayers is reflected by their phase behavior. For pure dipalmitoylphosphatidylcholine (DPPC) vesicles, it has been experimentally found that the phase transition temperature decreases with decreasing the diameter of the vesicle below a threshold value of $\simeq$ 70 nm.[2,3] The reason for this behavior is explained by the difficulty of lipid packing inside a strongly curved geometry. Experimental X-ray scattering data[4] show that the lateral density profile of a 80 nm diameter stearoyloleoylphosphatidylserine (SOPS) liposome exhibits structural asymmetry between the two monolayers. Due to differences in available packing space for the lipid tails between the inner and outer monolayer, the inner monolayer revealed a more disordered structure in comparison with the outer monolayer. From small-angle neutron scattering (SANS) studies[5,6] on PC liposomes exceeding 50 nm diameter it was concluded that the bilayer thickness decreases with increasing vesicle size. The

*Groningen Biomolecular Sciences and Biotechnology, Institute & Zernike Institute for Advanced Materials, University of Groningen, Nijenborgh 4, 9747 AG Groningen, The Netherlands. E-mail: S.J.Marrink@rug.nl*

 

interpretation of such scattering data has been questioned, however. In a subsequent combined X-ray/SANS/dynamical light scattering study[7] of the curvature effect on the structure of DOPC liposomes in the size range of 60–180 nm, no significant effect of curvature on either bilayer thickness or bilayer asymmetry was found.

Despite the importance of small vesicles, the structure of curved membranes at the level of molecular detail is still largely unresolved. Computer modeling studies could provide such detail, and studies of small vesicles are now computationally feasible. Important insights were already obtained, mainly for the self-assembly[8–11] and fusion[12–17] of small vesicles. Structural and dynamical aspects of vesicles remain largely unaddressed, however. Previously, we studied structural properties of highly curved ($<20$ nm diameter) PC–PE (phosphatidylethanolamine) mixed vesicles using a coarse-grained lipid model.[9] A small difference in lipid composition between the inner and outer monolayer was found, with the inner monolayer $\pm 2\%$ more populated with PE lipids than the outer monolayer. This observation is in line with the simple packing argument predicting that the inner monolayer prefers inverted-cone shaped lipids such as PEs. However, the data set in this study was very small and still within the range of a random distribution. Therefore, we extended this study with a more statistical significant data set which we present in the current manuscript. We consider three different systems: a pure DPPC liposome and two binary liposomes composed of DPPC : DPPE 1 : 1 and DPPC : DLiPC (dilinoleyl-PC) 1 : 1. Thus both the effect of a variation in the headgroup (PC *versus* PE) and a variation in the lipid tails (saturated palmitoyl *versus* polyunsaturated linoleyl) were studied independently. Relative to DPPC, DPPE and DLiPC are inverted cone shaped lipids characterized by a negative spontaneous curvature. In addition, we included the effect of temperature on the structural properties of the vesicles. Due to thermal motion within the tails, the optimal packing of the lipids within the monolayer and the distribution over the monolayers is expected to be temperature dependent. Special care was taken to equilibrate the vesicles. Right after their self-assembly, the vesicles were still unequilibrated and under considerable tension. We used artificial pores to allow lipid flip-flopping, required for the transmembrane composition of the vesicles to relax. The relaxation process took several 100s of nanoseconds, much longer than hitherto assumed by the simulation community.

The rest of this paper is organized as follows. In the next section, the simulation methodology is presented. The subsequent results and discussion section are split into two parts, the first part describing the (temperature-dependent) properties of pure DPPC liposomes, the second part dealing with the mixed liposomes. In the Appendix of this manuscript, we present a simple statistical model to describe transmembrane demixing of two-component vesicles.

## 2. Methods

### 2.1 Simulation setup

**CG-model.** All simulations were performed using the MARTINI coarse grained (CG) model of Marrink *et al.*[18,19] version 1.4. In this model small groups of atoms (four to six heavy atoms), are united into a single interaction center. Water is modeled explicitly, with one CG particle representing four real water molecules. The MARTINI model has been parameterized extensively, using a chemical building block principle. The key feature is the reproduction of thermodynamic data, especially the partitioning of the building blocks between aqueous and oil phases. Non-bonded interactions are described by a Lennard-Jones (LJ) potential. In addition to the LJ interactions, a screened Coulomb interaction is used to model the electrostatic interaction between the zwitterionic headgroups of the lipids. Connectivity and stiffness of the molecules is controlled by a set of standard bonded potential energy functions. Each of the three lipids used in this study (DPPC, DPPE, and DLiPC) are topologically identical in their CG representation. They consist of twelve beads, two for the headgroup, two for the glycerol linkage, and four for each tail. Although atomic detail is lost, the MARTINI model can still discriminate between lipids that differ in the chemical nature of either the headgroup or the tail. Distinctive membrane properties which strongly depend on the structural nature of the lipid, like the area per lipid, thickness[18,19] and even bending modulus[20] are well reproduced with the coarse grained model. To mimic the strong hydrogen bond donor capabilities of the ethanolamine compared to the choline moiety, a more polar CG particle type is used to represent the ethanolamine group.[18] With these parameters, the phase behavior of PC–PE lipid mixtures can be remarkably well reproduced.[21] The flexible character of the polyunsaturated linoleyl tail, on the other hand, is mimicked by the use of an appropriate set of angle potentials. These potentials were optimised with respect to the behavior of polyunsaturated tails observed in atomistic simulations of Feller *et al.*[22] From quantum mechanical calculations these authors concluded that polyunsaturated chains show an unusually high degree of conformational flexibility compared to monounsaturated or saturated chains. The same parameters were recently used in CG simulations[23] of the interaction of cholesterol and diarachidonoyl-PC, another $\omega 6$ fatty acid containing lipid, and in a simulation study[24] of domain formation in ternary mixtures of DPPC–DLiPC–cholesterol. For details of the lipid topologies and interaction parameters we refer to the original publications,[18,23] and to our web-site http://md.chem.rug.nl/coarsegrain.html.

**System details.** We used the MFFA-boundary potential method presented in the work of Risselada *et al.*[25] to simulate the liposomes more efficiently by reducing the number of degrees of freedom in the system. In here, the liposome is embedded in a spherical shell consisting of explicit solvent, eliminating excess water molecules that either surround the liposome or reside in the interior. Particles moving toward the boundary of the shell first experience a net attractive force. When particles approach the boundary more closely they experience a repulsive force. The strength of this repulsive force is soft in comparison to the normal pair wise Lennard-Jones interactions of the solvent. The nature of the mean field force potential is to compensate the surface tension at the boundaries which would otherwise occur in a system having a

finite size. The spherical symmetry of the MFFA boundaries has the additional benefit of a molding effect during the formation of liposomes, starting from a randomly distributed lipid mixture. It prevents the formation of some kinetically trapped intermediate aggregates during the process of liposome formation, resulting in very fast formation times ($\pm$10 ns). In our current set-up, the outer MFFA-boundary shell had a radius of 12.5 nm in all simulations performed. Due to the relative small internal volume of the liposomes of interest and therefore negligible gain in computational efficiency an inner boundary was not introduced. For a more precise specification of the method and its implementation we would like to refer to our previous work.[25]

All simulations were performed with a modified version of GROMACS-3.3[26] in which the MFFA-boundary method was implemented. The cut-off radius of both the MFFA-boundary and the pairwise interactions had a value of 1.2 nm. Shifted potentials were used for the non-bonded interactions, according to standard practice for the MARTINI force field.[18,19] The time step used in the simulation was 0.04 ps. Pressure and temperature were coupled to an external bath using the Berendsen coupling method ($\tau_P = \tau_T = 1.0$ ps$^{-1}$, $\beta = 5 \times 10^{-5}$ bar$^{-1}$).[27] The time scales quoted in the remainder of the manuscript are effective times, obtained by multiplication of the actual simulation time scale by a factor of four. This factor is based on the speed-up of the self-diffusion of water and lateral diffusion rate of lipids due to the neglect of atomic degrees of freedom.[18] However, the same factor need not apply to the processes described in the current manuscript. The time scales reported are therefore rather qualitative.

The systems studied are a pure DPPC liposome, a mixed 1 : 1 DPPC:DPPE liposome and a mixed 1 : 1 DPPC : DLiPC lipsome, all consisting of 2528 lipids and 43 303 CG water beads (corresponding to more than 170 000 real water molecules). The 1 : 1 composition has the advantage that at the start of the simulation the chance for a lipid to flip-flop from one to the other monolayer is equal for both species if the process would be random. Any deviation from random behavior then immediately points to a lipid-specific effect. To compare the structure of the liposomes with a normal bilayer, simulations of bilayers containing 512 lipids at the same compositions were also simulated. To investigate the effect of temperature on the liposomal membrane structure, we simulated each of the liposomes and planar bilayers at three different temperatures of 290 K, 323 K and 360 K. Note that the temperatures of 290 K is well below the experimental liquid-crystalline to gel phase transition temperature ($T_{main}$) for DPPC (at 315 K) and DPPE (335 K). The CG model also shows gel phase formation, albeit at slightly lower temperatures [$T_{main} = 295 \pm 5$ K for DPPC[28] and $T_{main} = 315 \pm 5$ K for DPPE (Risselada, unpublished work)]. The polyunsaturated DLiPC lipid remains fluid even at temperatures as low as 240 K. These values of the main transition temperature, experimental as well as computational, refer to lamellar systems. Strong curvature is expected to suppress the formation of a gel phase. Experimentally this effect has been observed for DPPC vesicles for which the phase transition temperature decreases with decreasing diameter of the vesicle.[2,3] For vesicles with a diameter of $\sim$35 nm, the transition temperature decreased by $\approx$5 K. For the vesicles $<$20 nm studied here, this effect is likely even larger, and explains the presence of a fluid liquid-crystalline phase for all of the liposomes studied. In fact, in a previous study from our group involving cooling of DPPC membranes[28] it was shown that gel phase formation in a DPPC vesicle requires a temperature drop to 265 K, well below the $T_{main}$ of the lamellar phase. Furthermore, it should be noted that CG models in general can not be expected to quantitatively reproduce the effect of temperature. Due to the very nature of coarse graining, the lack of entropy arising from the atomic degrees of freedom (especially from the solvent) is compensated with an effective enthalpic term. Temperature dependent properties should therefore be interpreted with care.

**Equilibration procedure.** Starting from a randomized distribution of lipids, sealed vesicles typically form on a time scale $<$10 ns, aided by the molding effect of the boundary potentials.[25] Due to the fast formation process, however, the transmonolayer lipid distribution is not equilbrated. This is remedied with the introduction of artificial hydrophilic pores, which allow a metastable liposome to relax to its lowest thermodynamic state.[25] Moreover, the flip-flop ratio between the two monolayers provides a useful criterion to determine the state of equilibrium of a given liposome. Artificial hydrophilic pores are formed by the addition of a repulsive harmonic potential ($K_{force} = 50$ kJ mol$^{-1}$ nm$^{-1}$) of cylindrical symmetry, which only acts on the carbon tails of the lipids. The radius of this cylindrically shaped boundary potential was set to 1.5 nm, large enough for the lipid head groups to line the pore forming a small water-filled transmembrane pore. As the length along the cylindrical boundary is 'infinite' (the system size), two pores occur in a liposome for each potential applied. In the pure DPPC liposomes, one potential was introduced (see Fig. 1). The cylindrical boundaries were present from the start of the self-assembly process, and were removed from the system after 800 ns allowing the membrane to seal.

Starting structures of the mixed systems were generated from the equilibrated DPPC liposomes (at the required temperature). To obtain the mixed liposomes exactly 50% of randomly chosen lipids in both monolayers of these DPPC liposomes were converted into either DPPE or DLiPC. Note that the alchemical transformation between the lipid species is trivial, as the lipids are topologically identical in the CG model used. After the conversion, three cylindrical boundary potentials were added to the system, resulting in the formation of six artificial pores allowing the mixed liposomes to equilibrate. For symmetry reasons the potentials were located along the three geometrical axis ($x$,$y$,$z$-axis) of the system. The larger number of pores in the mixed liposome was found to be required to equilibrate both the total transbilayer lipid distribution and transversal demixing of the two components. Still time scales for equilibration of some of the mixed systems exceeded 1 μs (see Results section). Each of the liposomal systems was simulated for another 20 ns after removal of the cylindrical potentials and sealing of the membrane, in order to collect data regarding the structural analysis.

 

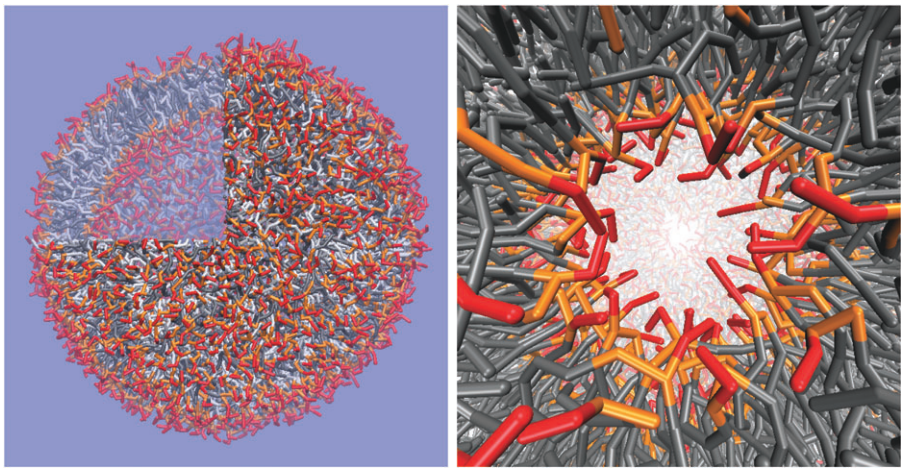

**Fig. 1** Impression of the structure of highly curved liposomes. The left figure shows an equilibrated DPPC–DLiPC 1 : 1 liposome after 400 ns of simulation at 360 K. A small cut in the liposome is made to highlight the inner membrane structure. The right figure shows a close up of the 'artificial' pore in a pure DPPC vesicle allowing its equilibration at 323 K. The lipid headgroups are located near the pore interface. In the back of the picture the second pore in the liposome is shown. The headgroups are colored red, glycerols orange, DPPC carbon tails grey and DLiPC carbon tails white. Water is not shown.

### 2.2 Analysis

**Structural properties.** The thickness of the bilayer was calculated from the difference between the average distance from all phosphate groups in the inner and outer monolayer to the geometrical center of the liposome. The second-rank order parameter $P2 = \langle\frac{1}{2}(3\cos^2\theta - 1)\rangle$ was computed for consecutive bonds with $\theta$ being the angle between the direction of the bond and the vector connecting the center of the bond with the center of the liposome. The area per lipid in a monolayer was defined based on the amount and position of the phosphate groups in the monolayer. As the liposomes were nearly spherical, the radius of the spherical shell in which the phosphate groups are located, $R_{\mathrm{av,mono}}$, is defined as the average distance of the phosphate-groups in the monolayer to the geometrical center. As the spread in the distribution of distances was found to be relatively small for the phosphate groups, within the approximation of a sphere the area of this spherical shell is defined as $A = 4\pi {R_{\mathrm{av,mono}}}^2$. The amount of lipids in a monolayer was determined using a criterion which includes the 'total' average radius $R_{\mathrm{av}}$ of the liposome. The average radius $R_{\mathrm{av}}$ was defined as the average distance of all phosphate groups (both inner and outer monolayer) to the center of the liposome, defining a lipid being located in the inner monolayer when the distance between the phosphate group and the center of the liposome is smaller than the average radius, and likewise a lipid being located in the outer monolayer when this distance is bigger than the average radius. Finally, the area per lipid is given as the area of the radial shell in which the phosphate groups are located divided by the amount of phosphate groups in the monolayer. The composition in a monolayer is given as the amount of lipids in a monolayer of a certain type divided by all the lipids in the monolayer. However, the precise amount of lipids in the monolayer can not be defined as long as the pores are present, therefore the presented numbers of lipid in the monolayer and compositions during equilibration times are an estimate.

**Dynamical properties.** The lipid flip-flop rate was calculated by identifying the location in the membrane of each lipid, *i.e.* inner *versus* outer monolayer, as a function time. To correct for the fluctuations at the pore interface introduced by this distance based criterion, a buffer region of 4 nm radius located around the center of the pore was defined. Only when a lipid was initially located in the monolayer outside the buffer region and it later appears in the other monolayer outside the buffer region it was counted as a flip-flop event. The lateral diffusion coefficient in the vesicle membrane was calculated from the mean square displacement on a spherical surface in which the lateral diffusion coefficient $D$ is given by, $D = \frac{\langle 4R^2\theta^2\rangle}{t}$, where $\theta$ is the angle between the membrane normal vector at $t = 0$ and $t = t$, defined as the connecting vector between the center-of-mass of the vesicle and the center-of-mass of the lipid, and $R$ is the radius of the vesicle. In this study the diffusion was fitted from the mean square displacement between 5 and 50 ns. To correct for the overall motion of the monolayers in the vesicle, both linear- and angular rigid body momentum were removed at each iteration step for each monolayer separately. To further characterize the fluidity of the membrane in terms of its local dynamical properties the reorientational auto-correlation function $C(t)$ of the P2 order parameter was calculated. The plateau of $C(t)$ at long times corresponds to a residual value and reflects the long time order of the system.

## 3. Results and discussion

We will now describe and discuss our results, first those obtained for pure DPPC liposomes followed by the results for the mixed liposomes. For both systems we start with a description of the equilibration process of the liposomes. Subsequently the structural properties of the equilibrated liposomes are characterized in detail, including their temperature dependency. Table 1 gives an overview of the various properties of the liposomes, together with results for a pure DPPC bilayer for comparison.

**Table 1** Structural properties of the pure and mixed liposomes

| | $d$/nm[bc] | $R$/nm[bc] | $N_{in}$ | $N_{out}$ | $N_{in}/N_{out}$ | In frac.[a] | $A_{in}$/Å$^{2bc}$ | $A_{out}$/Å$^2$ | $A_{in}/A_{out}$ |
|---|---|---|---|---|---|---|---|---|---|
| DPPC liposome: | | | | | | | | | |
| 290 K | 4.17 | 7.92 | 910 | 1618 | 0.56 | — | 47.0 | 77.7 | 0.60 |
| 323 K | 3.97 | 8.20 | 935 | 1593 | 0.57 | — | 51.9 | 81.8 | 0.63 |
| 360 K | 3.83 | 8.54 | 958 | 1570 | 0.61 | — | 57.6 | 87.5 | 0.66 |
| DPPC bilayer: | | | | | | | | | |
| 290 K | 4.43 | — | 256 | 256 | 1 | — | 56.4 | 56.4 | 1 |
| 323 K | 4.14 | — | 256 | 256 | 1 | — | 62.1 | 62.1 | 1 |
| 360 K | 3.88 | — | 256 | 256 | 1 | — | 68.0 | 68.0 | 1 |
| DPPE : DPPC liposome: | | | | | | | | | |
| 290 K | 4.19 | 7.70 | 936 | 1592 | 0.59 | 0.56 | 41.2 | 76.8 | 0.54 |
| 323 K | 4.02 | 8.01 | 953 | 1575 | 0.61 | 0.59 | 45.8 | 82.1 | 0.56 |
| 360 K | 3.93 | 8.27 | 978 | 1550 | 0.63 | 0.59 | 50.1 | 86.2 | 0.58 |
| DliPC : DPPC liposome: | | | | | | | | | |
| 290 K | 3.91 | 8.09 | 954 | 1574 | 0.61 | 0.51 | 48.6 | 81.6 | 0.60 |
| 323 K | 3.74 | 8.46 | 971 | 1557 | 0.62 | 0.51 | 51.9 | 88.2 | 0.59 |
| 360 K | 3.69 | 8.67 | 993 | 1535 | 0.65 | 0.52 | 57.6 | 92.0 | 0.63 |

[a] The fraction of inverted cone shape lipids in the inner monolayer of the liposome. [b] The area per lipid ($A$), radius ($R$) and thickness ($d$) are based on the average position of all phosphate groups in a monolayer. The radius is defined as the center between the radial density peaks of the phosphates in both monolayers. [c] The errors are within 1% of the average values.

### 3.1 Pure DPPC liposomes

**Lipid flip-flop required for liposome equilibration.** Fig. 2A shows the amount of DPPC lipids in the inner monolayer as a function of time for the three temperatures. After starting the simulations the DPPC lipids quickly self-assemble into porated liposomes. The pores were kept open artificially by the presence of a cylindrical boundary potential as described in the Methods section. The liposomes are formed fast, aided by the molding effect of the spherical boundary potential surrounding the system. Formation times are 80 ns, 40 ns and 25 ns at 290 K, 323 K and 360 K, respectively. In Fig. 2A the formation times are roughly corresponding to the time were the initial steep behavior (0–80 ns) ends. The shorter formation times at elevated temperatures can be attributed to enhanced lipid diffusion rates. Due to the fast kinetics of the self-assembly process, lipid monolayers are not equilibrated after the formation of the liposome. Further equilibration is reached by lipid flip-flop through the pores. In Fig. 2A, a clear change is seen to take place over the first 100s of nanoseconds, resulting from a net movement of lipids from the outer toward the inner monolayer. Although there might be still small systematic trends present throughout the entire simulation time, equilibrium is roughly reached after 200–300 ns in each of the systems. After the equilibration period, flip-flops still occur (showing up as fluctuations in the graphs of Fig. 2), but net transport of lipids is no longer taking place.

Fig. 2B presents a more detailed analysis of the amount of pore-mediated flip-flops in case of the DPPC liposome at $T = 323$ K. Flip-flops are detected from $t \approx 200$ ns, and separated between inner-to-outer monolayer 'flips' and outer-to-inner monolayer 'flops'. The flip-flops are further distinguished with respect to the pore (upper or lower) through which they pass, to get a feeling for the statistical significance of the events. Based on the curves obtained for the two pores independently, a spread of approximately 10 lipids over the whole trajectory reflects the statistical uncertainty in the number of observed flip-flops. The overall difference in the number of flip-flops between the flip and flop direction is similar, hence can be attributed to the stochastic nature of the process. The slope of the curve is proportional to the flip-flop rate. Although the slope still seems to increase a bit during the 200–300 ns time period, a constant value is reached for the remainder of the simulation. The estimated flip-flop rate per pore $J_f = 0.1 \pm 0.01$, $0.2 \pm 0.02$ and $0.4 \pm 0.02$ ns$^{-1}$ at 290, 323 and 360 K, respectively. The temperature effect can again be explained from the increased diffusion rate of lipids at higher temperatures. In addition, an increased temperature helps to overcome an energetic barrier which might exist at the pore interface. The rates obtained with our CG model are somewhat larger compared to pore-mediated flip-flop rates observed in atomistic studies,[11,29,30] ranging from 0.1 ns$^{-1}$ to 0.02 ns$^{-1}$ at 323 K. The obtained differences in flip-flop rate might be due to differences in the nature of the pore (*e.g.* size) or due to approximations underlying the CG model.

**Curvature induces membrane thinning and reduces thermal expansivity.** Table 1 shows that the curved membrane of the liposome is thinner than the non-curved planar membrane. The thickness of the liposomal membrane is 94%, 96% and >99% of the thickness of the lamellar system, at 290 K, 323 K and 360 K, respectively. The relative difference in thickness is decreasing with increasing temperature and becomes insignificant at 360 K. At least part of this effect is due to the increasing overall radius of the liposome, reducing its curvature. The bilayer thickness in the liposome increases from 3.83 nm at 360 K to 4.17 nm at 290 K, which is around 9%. The lamellar bilayer thickness increases over the same temperature range from 3.88 nm to 4.43 nm, around 14%. Therefore, the relative increase in membrane thickness due to the decrease in temperature is significantly smaller in the curved membrane than in the non-curved membrane. In other words, curvature induces membrane thinning, and reduces the thermal expansivity. Likely these two effects are related, as an already thinned membrane has fewer options to further expand. Interestingly, the bilayer thinning we see here, as well as in our previous study,[9] contrasts experimental data which

 

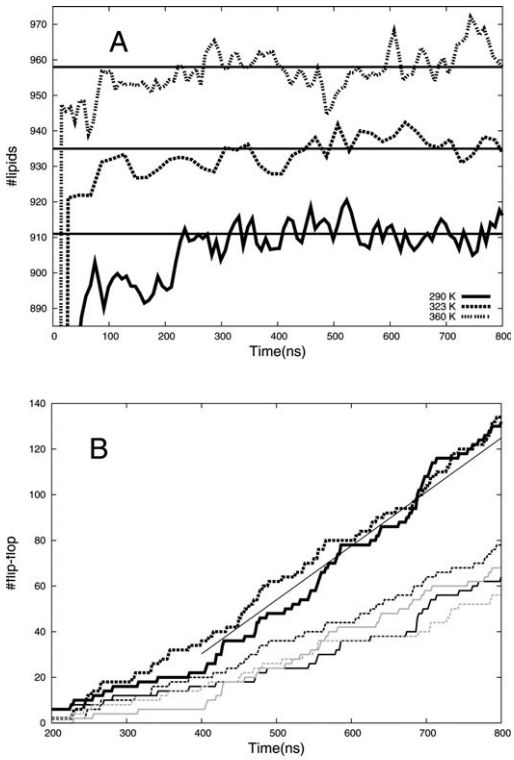


**Fig. 2** (A) Equilibration of liposomes by pore-mediated lipid flip-flops. The graphs represent the amount of lipids in the inner monolayer of the liposome as a function of time, at three different temperatures. The liposomes self-assemble in 10s of nanoseconds. It takes approximately 300 ns for the liposomes to fully equilibrate. Trend lines indicating the equilibrium composition are added at $y = 911$ (290 K), $y = 934$ (323 K), and $y = 958$ (360 K). (B) Number of flip-flops as a function of time in the pure DPPC liposome at 323 K. Due to the used analysis criterion (see Methods section) the first flip-flops are detected after 200 ns. Solid lines represent the flip-flops from outer monolayer to the inner monolayer and dashed lines the flip-flops from the inner to the outer monolayer. Thick black lines represent the total amount of flip-flops in the liposome. Thin black lines represent the flip-flop events through the upper and thin grey lines the flip-flop events through the lower pore in the liposome. The thin black straight line indicates the average constant flip-flop rate (0.2 $ns^{-1}$).

suggest either no effect[7] or even an increasing bilayer thickness upon increasing curvature.[5,6] However, the experiments probe vesicle sizes exceeding 60 nm, whereas our simulated vesicles are 20 nm in diameter. The size and hence curvature difference and/or the use of different lipids could explain the difference in observed thinning behavior.

**Higher temperatures favor more symmetrically populated monolayers.** Whereas in a lamellar system the two monolayers are indistinguishable, at least for a one component bilayer, this is no longer the case in a liposomal system. Table 1 shows that in the liposome the area per lipid, at the level of the phosphate headgroups, is larger in the outer compared to the inner monolayer. In fact, the area per lipid of the outer liposomal monolayer at 290 K, 77.7 $Å^2$, is even much larger than the area per lipid of the normal bilayer at 360 K, 68.0 $Å^2$. The headgroups in the inner monolayer, on the other hand, are packed at high temperature (360 K) similar to the headgroups of a lamellar membrane in a supercooled state (55 $Å^2$ at 283 K).[28] The area per lipid in the inner monolayer is, respectively, 60%, 63% and 66% of the area per lipid of the outer monolayer at 290 K, 323 K and 360 K, showing a decrease in the difference in area per lipid between the two monolayers at increasing temperature. This trend seems related to the increase in symmetry in monolayer population at increased temperatures. Table 1 shows that the amount of lipids in the inner monolayer and the amount of lipids in the outer monolayer become more equal with increasing temperature, implying that the monolayer becomes more symmetrically populated ($N_{in}/N_{out}$ increasing). This effect could be due to two reasons: (i) at increasing temperature the radius of the liposome increases, therefore the curvature difference between the two monolayers decreases and they become more symmetrically populated; or (ii) at higher temperatures the effective volume of the tails increases due to the increased thermic motions, making the lipids effectively more inverted cone shaped. Due to a more efficient packing of inverted cone shaped lipids in the inner monolayer (negative curvature), the lipids have a relative higher tendency to occupy the inner monolayer. The packing subtleties are further discussed below.

**Lipid packing in inner *versus* outer monolayer is very different.** The radial density profile in Fig. 3 reveals that the density in the headgroup area is larger in the inner monolayer than in the outer monolayer of the liposome. In contrast, the density of the carbon tails is larger in the outer monolayer than in the inner monolayer. These two effects can be explained by simple packing arguments, dictated by the constraints posed by the liposomal geometry. The convex volume occupied by the lipid tails in the outer monolayer forces them to pack closer, *i.e.* at higher density, compared with the tails in the inner monolayer that occupy a concave volume element. On the other hand, the headgroups of the outer monolayer have relatively more available packing space than the headgroups of the inner monolayer, resulting in the opposite effect. From the overlap of the water peak with the phosphate peak in Fig. 3, it is furthermore concluded that the hydration level of the outer monolayer is larger (full overlap) than the hydration level of the inner monolayer (partly overlap). The large space available to the lipid headgroups in the outer monolayer allows them to be solvated completely, whereas the limited space in the inner monolayer causes dehydration. Interesting is also the distribution of the ends of the lipid tails, showing a more narrow and symmetric peak for the inner monolayer compared to the outer monolayer. The broad asymmetric peak of the tail beads in the outer monolayer was previously[9] shown to be caused by an increased 'back-folding' behavior of the lipid tails toward the center of the head group region. The backfolding of lipid tails makes use of the relative low density headgroup region, thereby avoiding the overly crowded bilayer center.

The effect of temperature on the radial density distribution can be assessed by comparison of the profiles obtained at high temperature (360 K) *versus* low temperature (290 K). Fig. 3 shows a clear decrease in overall membrane density at increasing temperature, together with a shift of the peaks reflecting the increased radius of the thermally expanded liposome. The

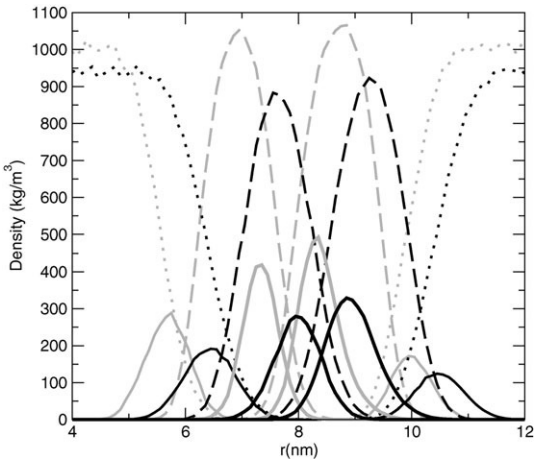


**Fig. 3** Distribution of components across the liposomal systems. The radial density of the liposome membrane at 360 K (black) and 290 K (grey) is shown with respect to the center-of-mass of the liposome ($r = 0$). Thin solid lines are representing the phosphate headgroups, thick solid lines the last tail beads (C4), dashed lines the carbon tails and dotted lines water. The carbon tails are plotted separately for each monolayer.

reduced hydration of the inner monolayer and the backfolding of the outer monolayer tails are more pronounced at low temperature, presumably caused by the increase in curvature radius.

Fig. 4 shows the P2 local order parameters for the DPPC liposomes at the three different temperatures. From these data it can be concluded that the tail bonds are more disordered in the inner membrane leaflet compared to the outer leaflet. The bonds between the phosphate-group (PO4) and the first glycerol group (GLY1), however, show an increased order. These findings corroborate the conclusions drawn above, based on the radial density distribution. Tails are more ordered and thus more tightly packed in the outer monolayer. Toward the head group region this trend is reversed. In line with expectations, at increasing temperature the overall order in the tail region in both monolayers decreases. The headgroup region shows less temperature dependency; the bond vector between the choline group (NC3) and phosphate group (PO4) and the bond vector between the two glycerol groups (GLY1 and GLY2) remain rather constant. Apparently, the tails of lipids have more internal degrees of freedom to respond to curvature constraints and/or changes in temperature.

**Dynamical properties in the vesicle membrane differ between the monolayers.** Fig. 5 shows the lateral diffusion rate of lipids in the pure DPPC vesicle at 290 K and 360 K considering different parts of the lipid separately. For small liposomes the lateral diffusion of lipids can not be uniquely defined since the lateral displacement within a lipid is locally dependent on the distance to the liposome center. Fig. 4 shows that the lateral diffusion coefficients are between 1–2.2 $\times$ $10^{-7}$ cm$^2$ s$^{-1}$ at 290 K and 4–7.7 $\times$ $10^{-7}$ cm$^2$ s$^{-1}$ at 360 K. The diffusion coefficient found at 290 K lies within the experimental estimated range of 1 $\times$ $10^{-8}$ to 2 $\times$ $10^{-7}$ cm$^2$ s$^{-1}$ found for 20 nm phospholipid vesicles at 305 K.[31] Fig. 5 also reveals that although the lateral diffusion in absolute space seems faster for lipids in the

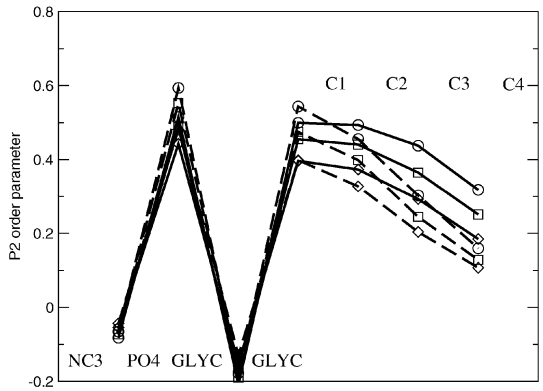


**Fig. 4** Local order parameters (P2) in the liposomal DPPC membrane at three different temperatures. Solid lines represent the outer monolayer, dashed lines represent the inner monolayer. Circles represent 290 K, squares 323 K and diamonds 360 K. The standard error in the order parameter lies within the resolution of the depicted points.

outer monolayer, the lateral diffusion in angular space in fact reveals the opposite. Using the value of the diffusion coefficient of the phosphate group in the inner monolayer as a reference, correction for the radius dependency (grey line Fig. 5) reveals that the individual beads in the lipid indeed possess the same angular displacement. It also reveals, however, that the angular displacement of lipids is larger in the inner monolayer compared to the outer monolayer and that this difference increases with increasing temperature. In practice this means that the inner monolayer is sampled faster by the lipids than the outer monolayer. Compared to the planar membranes the diffusion rate in curved membranes appears significantly slower. From our simulations we calculate the lateral diffusion coefficients of lipids in the planar membrane to be, 2.7 $\pm$ 0.3 cm$^2$ s and 11.8 $\pm$ 1.9 cm$^2$ s at 290 K and 360 K, respectively, almost twice as fast.

To see if the lipid dynamics in liposomes is generally slower, we also calculated the auto-correlation function of the P2 order parameter of the carbon tails for both the pure DPPC vesicle and the planar DPPC bilayer. Fig. 6 shows the results,

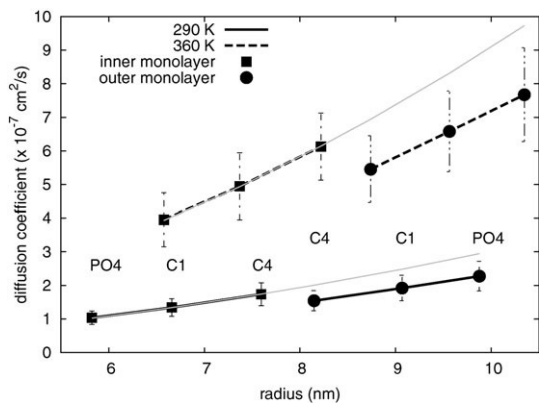


**Fig. 5** Lateral diffusion coefficient of lipids in the liposomal DPPC membrane at 290 K and 360 K, separated for different parts of the lipids. The grey line is a correction for the radius dependence in the lateral diffusion $D$, $D(r) \propto r^2$, which corresponds to a constant mean square angular displacement $\langle\theta^2\rangle$.

 

revealing the following two main features: (i) the relaxation time of the tails increases with increasing curvature. This finding agrees qualitatively with the experimental work of Lepore *et al.*[32] in which a small but significant increase in the relaxation times of the tails was found in 35 nm diameter vesicles compared with 90 nm diameter vesicles, most notable in the vicinity of the lipid headgroup. The more pronounced influence of curvature on tail dynamics in this study is most likely attributable to the large difference in curvature and resulting tail order parameter between the planar membrane and the 20 nm diameter vesicle; (ii) the reorientation dynamics of the lipid tails is faster in the inner monolayer, especially for the lower-temperature case. This finding is in agreement with the faster angular diffusion of the lipids in the inner monolayer as concluded in the preceding paragraph, and is likely related to the larger packing volume and more disordered state of the lipid tails in the inner monolayer. In summary, we find that lipid dynamics is slowed down in liposomes compared to planar membranes, and that this is caused mainly by the increase in lipid tail density of the outer monolayer.

### 3.2 Mixed liposomes

**Lipid flip-flops induce transversal demixing in mixed liposomes.** The mixed systems (DPPE–DPPC and DLiPC–DPPC) were generated from the pure DPPC liposomes. Six artificial pores were added to allow for the subsequent transmonolayer equilibration process. In addition to the total number of lipids in each monolayer, also the relative concentrations of both lipid species in each of the two monolayers needs to equilibrate. Fig. 7 shows the ratio of the concentrations in the inner monolayer as a function of time. Starting from the initial unbiased 1 : 1 ratio (*i.e.* equal concentrations of both lipids in each monolayer), the increase of the relative concentration of the inverted cone shape lipids (DPPE and DLiPC) in the inner monolayer is observed.

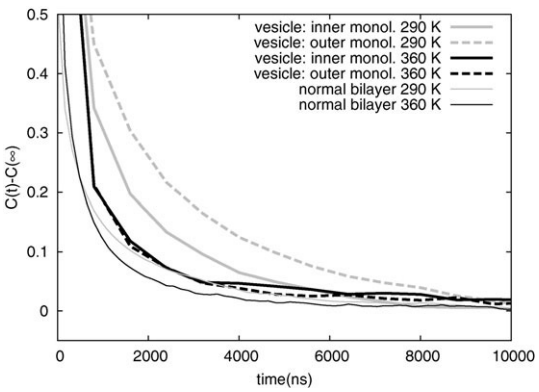


**Fig. 6** Auto-correlation function $C(t)$ of the P2 order parameter of the pure DPPC vesicle at 290 K (grey lines) and 360 K (black lines). The P2 order parameter is calculated from the angle of the vector connecting the first (C1) and last (C4) carbon tail bead with the local membrane normal vector. The auto-correlation function of the vesicle (thick lines) is compared with the auto-correlation function of the normal membrane (thin lines). For the vesicle, the auto-correlation function is separately calculated for the lipids in the inner (solid lines) and outer (dashed lines) monolayer of the vesicle. To compare the different situations, the ensemble average of the P2 order parameter, $C(\infty)$, is subtracted from each point.

This is true for each of the three temperatures studied. The increase in concentration of inverted cone shape lipid in the inner monolayer is stronger for DPPE than for DLiPC. Almost independent of temperature, the DPPE concentration in the inner monolayers drifts towards 60%, while only around 51% is reached for the polyunsaturated lipid. In the case of DLiPC, this value is already reached either during or right after the formation of the artificial pores. The value of 51%, however, falls within the statistical spread expected for a binary mixture with no particular preference of either lipid for any of the two monolayers (see Appendix for details). The upward drift of the DPPE concentration in the inner monolayer shows signs of saturation after around 1 μs of simulated time, although it can not be excluded that a systematic drift is still present at the end of the simulation. The reason for the stronger transmonolayer demixing for DPPE *versus* DLiPC becomes apparent when we discuss the lipid packing later on.

**Mixed liposomes have a more symmetric transmonolayer distribution of the total lipid amount.** Structural properties of the mixed liposomes are given in Table 1, including the total numbers of lipids in the inner and outer monolayer as well as the ratio between them, and the area/lipid in both inner and outer monolayer. From these results it is concluded that the inverted cone shape lipids enhance the symmetry in lipid population between the monolayers. Overall, the monolayers are more equally populated by lipids for both of the mixtures compared to the pure DPPC liposomes, at a given

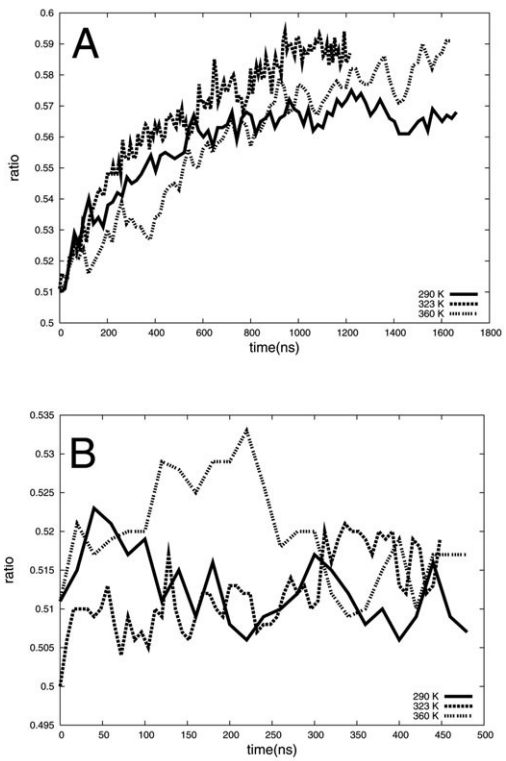


**Fig. 7** Enrichment of the inner monolayer by inverted-cone shaped lipids. The ratio of DPPE (A) or DLiPC (B) in the inner *versus* the outer monolayer is plotted as a function of simulation time. Results are shown for the three temperatures of study.

temperature. The effect seems significantly stronger for the DLiPC lipids than for DPPE. The latter observation can be explained by the difference in size of the liposomes. The mixed DPPE–DPPC liposomes are smaller than the mixed DLiPC–DPPC liposomes, their radii differing by $\approx 0.4$ nm. The size difference, in turn, is explained by the relative small area per lipid adopted by PE lipids *versus* the polyunsaturated PC lipids. The size of the DPPC liposomes is in between. Yet the asymmetry in the population numbers is largest in this case. The reason for this additional effect can be found in the transversal demixing observed in the mixed systems. As the inner monolayer favors inverted-cone shaped lipids, the fraction of DPPE or DLiPC lipids is enhanced in the inner monolayer, leading to a more symmetric overall lipid distribution. Especially for DPPE this effect is apparently strong enough to overcompensate for the size effect. Somewhat surprisingly, the extent of demixing appears rather insensitive to the temperature. This observation leads us to conclude that the overall effective shape of the lipids, which governs their ability to pack inside curved membranes, remains more or less the same over the temperature range studied.

**Lipid packing in mixed liposomes: competition between shape and flexibility.** Analogous to our analysis of the packing of the lipids in pure DPPC liposomes, for the mixed systems we also calculated both the order parameter profiles and the density distribution functions. Fig. 8 shows the P2 order parameters of the mixed liposomes in comparison with a pure DPPC liposome. The general difference in order parameters observed between the inner and outer monolayer, most notably the larger disorder of the lipids tails in the inner monolayer (*i.e.* lower order parameters), is also present in the mixed systems. The differences between the lipid order in the pure and mixed liposomes are mostly subtle. In fact the DPPC lipids show quantitative very similar profiles regardless of the overall composition. The effect of the unsaturated bonds in DLiPC (Fig. 8B) shows up in the decreased order of the tail bond vectors.

Fig. 9 shows the radially averaged density profiles of the liposomal membrane, for both mixed liposomes. The Figure reveals an asymmetric distribution in overall density between the bulk peak of DPPC and DPPE, and to a lesser extent between DPPC and DLiPC, arising from the transversal demixing between the two monolayers. In order to compare the relative packing of the lipids, the separated profiles for the lipid head group, tails and terminal tail group were normalized with respect to the monolayer concentration of each lipid species. For both the DPPC–DPPE and the DPPC–DLiPC system, almost no difference is observed between the relative densities of the sub-components of both lipids in the respective monolayers. This is in agreement with the lack of a large effect on the order parameter profiles as discussed before. To a first approximation, both lipids are packed in a similar way. However, on closer view, some subtleties can be discerned that are of importance. Comparing the profiles for DPPC and DPPE (Fig. 9A), it appears that the PC lipids are shifted a little more toward the bilayer interfaces, whereas the PE lipids

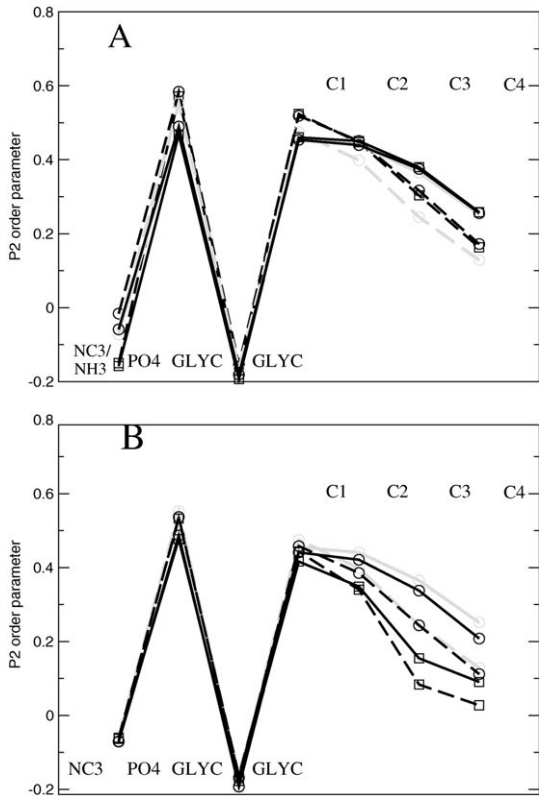


**Fig. 8** Order parameters (P2) of the equilibrated mixed liposomes in comparison with a pure DPPC liposome. Panel (A) shows results for the DPPE–DPPC liposome, panel (B) for the DLiPC–DPPC liposome, both at 323 K. Solid lines represent the outer monolayer, dashed lines the inner monolayer. Circles denote the DPPC lipids, squares either DPPE or DLiPC. The grey lines represent the order parameters of the pure DPPC liposome at the same temperature. The standard error in the order parameter lies within the resolution of the depicted points.

sample more of the interior space. We understand this effect as arising from the larger tendency of PC lipids to be hydrated in comparison to the PE lipids which form intra-lipid hydrogen bonds more easily. (Note: although the CG model used here does not consider explicit hydrogen bonds, the average effect of hydrogen bonding is taken into account.) This explanation is supported by other studies concerning atomistically detailed simulations of mixed PE–PC bilayers.[33,34]

In the mixture of DPPC–DLiPC (Fig. 9B) the relative density of the headgroups is almost identical, as is the chemical structure of their head groups. Here a small but significant difference is seen in the density profile of the tails. In comparison to DPPC, the tail profiles for DLiPC are shifted toward the exterior of the liposome. Whereas in the case of the DPPC–DPPE liposome the shift of the profiles is symmetric with respect to the membrane center, for DPPC–DLiPC the shift is asymmetric. These results can be explained as follows. In the outer monolayer, back-folding of the lipid tails is advantageous as it releases the packing stress near the bilayer center. Poly-unsaturated chains are much more flexible compared to saturated chains, and are therefore more amenable to back-folding. This shows up most clearly in the profiles of the

 

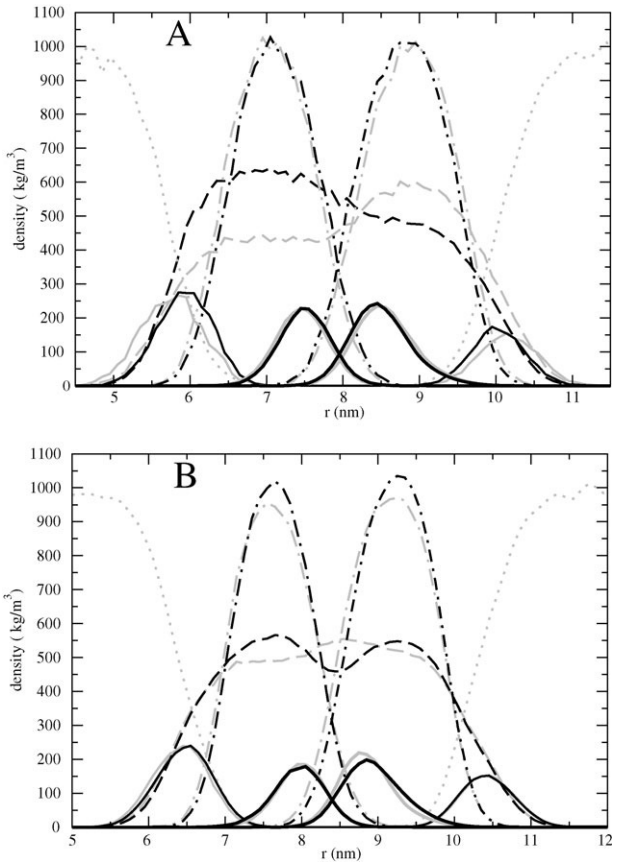


**Fig. 9** Radial density profile of the liposome membrane for both mixed liposomes. The radius is calculated with respect to the center-of-mass of the liposome. (A) DPPC–DPPE liposome and (B) DPPC–DLiPC liposome, both at 323 K. Grey colors represent DPPC. Black colors represent either DPPE or DLiPC. Thin solid lines represent the phosphate head groups, thick solid lines the last tail beads (C4-group), dotted lines water, dotted-dashed lines the carbon tails and long dashed lines the total contribution for each lipid component. In order to compare the relative densities, the phosphate groups, C4-groups and the carbon tails are independently normalized relative to the population of the lipid type in each monolayer.

terminal tail group, which is broadened toward the interface in case of DLiPC. The back-folding ability of polyunsaturated lipids is also seen in atomistic simulations.[35] In fact, the CG model for the polyunsaturated chains has been parameterized based on these simulations, as described in.[23] In the inner monolayer, back-folding is not required as it would only increase the density at the already crowded interface. Here the DPPC density near the interface is somewhat larger due to the fact that the saturated lipids are effectively longer (*i.e.* less disordered tails), causing them to stick out of the interface. As a consequence of the more ordered conformation of the saturated lipids and the back-folding of the polyunsaturated lipids in the outer monolayer, an increased density of DPPC in the membrane interior is also noticeable.

The subtle packing details of the polyunsaturated tails may also explain why the expected enrichment of DLiPC in the inner monolayer is so minor (51% as opposed to almost 60% for DPPE). Based on the shape model only, the inner monolayer should be clearly favored for accommodating the inverted-cone shaped DLiPC lipid. The back-folding ability of DLiPC actually provides a counter-acting driving force for the lipid to reside in the outer monolayer. Given the close to even distribution of DPPC and DLiPC in each of the two monolayers, the two opposing forces seem more or less equal. Our observation of this remarkable feature adds another possible role of polyunsaturated lipids in biological membranes. In addition to its claimed role in stabilizing membrane proteins,[36,37] the formation of fluid, cholesterol depleted domains,[38,39] and the ability to trigger membrane fusion,[40,41] we speculate that polyunsaturated lipids may be used for their ability to stabilize both negative and positive regions of curvature.

In summary, Fig. 10 shows a schematic picture of the packing of the different lipid components in curved bilayers, based on the results presented in the current manuscript. Packing of lipids in small liposomes can not solely be described by a static shape concept, but also requires the flexibility of the lipids to alter their shape to be taken into account.

## 4. Appendix: statistical model

If one considers an ensemble of equilibrated binary mixed liposomes, what would be the statistical distribution of the two lipid components in both inner and outer monolayer? To get insight in the statistical properties of such an ensemble, a simple statistical approach is presented here. Let $N$ be the total number of lipids in the liposome. Now $N_A$ is the number of lipids of type A (cone shaped) and $N_B$ of type B (inverted cone shaped). For simplicity we consider a constant number of lipids in the inner and outer monolayer such that $N_{in}^{A} + N_{in}^{B} = N_{in}$ and $N_{out}^{A} + N_{out}^{B} = N_{out}$ with $N_{in} \leq N_{out}$. The ratio $N_{in} : N_{out}$ represents the curvature in a bilayer. The relative preference for lipids of type A to be in the outer monolayer is denoted $p_{ex}$; The preference for the inner monolayer is then given by $1 - p_{ex}$. Similarly, for the lipid of type B the probabilities are $1 - p_{ex}$ and $p_{ex}$ for the outer and inner monolayer respectively. For $p_{ex} = 0.5$ both lipids are of the same type. Starting from a random distribution of type A and B lipids over both monolayers, lipids are randomly selected to undergo exchange events. Weighted according to the monolayer preferences ($p_{ex}$ or $1 - p_{ex}$), a lipid is exchanged with a lipid from the opposing monolayer. In practice this requires a limited amount of numerical iterations to reach equilibrium conditions. Equilibrium is reached when the intrinsic probability to exchange a certain lipid type is counteracted by the probability to select this lipid type. Using this simple statistical analysis, the effect of curvature on the distribution of lipids can be evaluated.

Fig. 11 shows probability distributions of the composition (number) of inverted cone shaped lipids which can be found in the inner monolayer of a liposome under various conditions. It becomes clear that the effect of transversal demixing ($p_{ex} > 0.5$) itself only affects the position of the distribution and not the width of the distribution. On the other hand, asymmetry ($N_{in} : N_{out}$) only influences the width of the distribution and

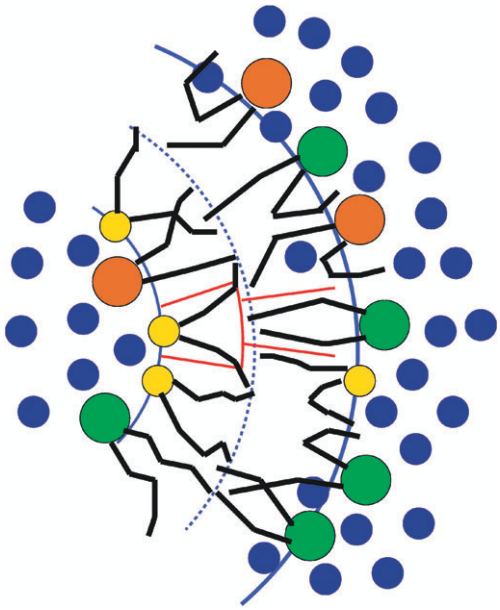

**Fig. 10** Schematic drawing of the molecular packing of lipids in small mixed liposomes. The blue lines represent the position of the water/lipid interface (solid) and geometrical bilayer center (dashed). The average volume element occupied in either monolayer (concave—inner monolayer, convex—outer monolayer) is shown in red. Dark blue circles represent water, green circles the DPPC headgroups, gold circles the DPPE headgroups, and brown circles the DLiPC headgroups. The following features are visualized: (i) the headgroups in the outer monolayer are more hydrated than the headgroups in the inner monolayer; (ii) PE headgroups are located more closely toward the center of the membrane and are therefore less hydrated than the PC headgroups; (iii) in the inner monolayer the tails are more disordered; (iv) the inner monolayer is enriched in DPPE lipids which dehydrate more easily in response to the smaller volume available at the water/lipid interface; (v) in the outer monolayer all lipid types show either increased back-folding of the tails or penetration beyond the bilayer center; (vi) the polyunsaturated tails of DLiPC show more frequent back-folding than the tails of the other lipid components; (vii) DLiPC does not have a strong affinity foreither monolayer, because although DLiPC is an inverted-cone shaped lipid, the back-folding of the tails counteracts the packing constraints caused by the bulkiness of the polyunsaturated tails.

not the position of the median. Furthermore, the width of the distribution in a binary mixture is also dependent on the composition. The distribution shows a maximal width for a symmetric 1 : 1 inverted cone shaped : cone shaped lipid mixture. Purely on statistical bases the probability distribution of the number of inverted cone shaped lipids present in the inner leaflet of liposomes is expected to show broadening with increased liposome curvature. For a 1 : 1 binary mixed symmetric bilayer (1256 : 1256) a monolayer composition between 0.490 and 0.510 ($\sigma$ = 0.010) of one lipid type lies still within the standard deviation $\sigma$ of a random distribution. For a typical 1 : 1 binary mixed liposomes (940 : 1588) used in this study, these values are between 0.487 and 0.513 ($\sigma$ = 0.013). This implies that insights in the effect of transversal demixing from an ensemble of small spontaneously formed liposomes would require a larger statistical data set especially when the effect is small. The demixing seen in our simulations for

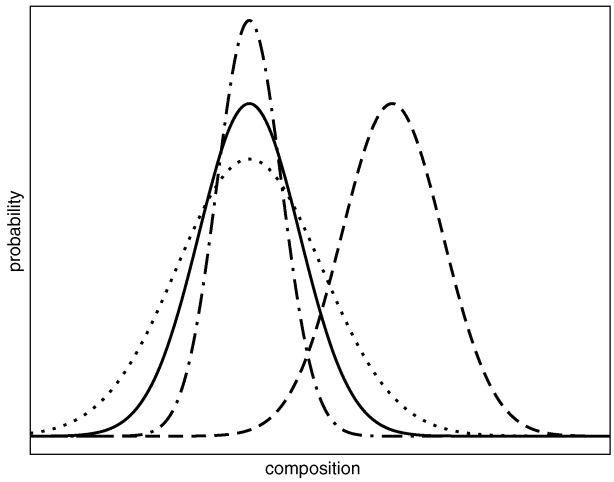


**Fig. 11** Probability distributions of the composition (number) of inverted cone shaped lipids found in the inner monolayer of liposomes. The solid line represents a random ($p_{ex}$ = 0.5) lipid distribution of a 1 : 1 (overall composition) inverted cone shaped : cone shaped lipid mixture in a normal symmetric bilayer. The dotted line represents a random lipid distribution for the same mixture in a curved bilayer. The long dashed line represents a non-random ($p_{ex} \neq 0.5$) lipid distribution for the same mixture in a curved bilayer. The dotted-dashed line represents a random lipid distribution for an asymmetric overall membrane composition (*e.g.* 1 : 2 inverted cone shaped : cone shaped lipid mixture) in a normal symmetric bilayer. The distribution is shifted to compare the difference with a distribution of a 1 : 1 inverted cone shaped : cone shaped lipid mixture.

DPPC–DPPE is statistically significant, the demixing seen for DPPC–DLiPC falls within the limits of random mixing.

## References


1 B. A. Cronell, G. C. Fletcher, J. Middlehurst and F. Separovic, *Biochim. Biophys. Acta*, 1982, **690**, 15–9.
2 R. L. Biltonen and D. Lichtenberg, *Chem. Phys. Lipids*, 1993, **64**, 129–142.
3 R. Koynova and M. Caffrey, *Biochim. Biophys. Acta*, 1998, **1376**, 91–145.
4 M. R. Brzustowicz and A. T. Brunger, *J. Appl. Crystallogr.*, 2005, **38**, 126–131.
5 M. A. Kiselev, E. V. Zemlyanaya, V. K. Aswal and R. H. H. Neubert, *Biophys. Lett.*, 2006, **35**, 477–493.
6 H. Schmiedel, L. Almasy and G. Klose, *Biophys. Lett.*, 2006, **35**, 181–189.
7 N. Kucerka, J. Pencer, J. N. Sachs, J. F. Nagle and J. Katsaras, *Langmuir*, 2007, **23**, 1292–1299.
8 H. Noguchi and M. Takasu, *Phys. Rev. E*, 2001, **64**, 41913.
9 S. J. Marrink and A. E. Mark, *J. Am. Chem. Soc.*, 2003, **125**, 15233–15242.
10 A. J. Markvoort, K. Pieterse, M. N. Steijaert, P. Spijker and P. A. J. Hilbers, *J. Phys. Chem. B*, 2005, **109**, 22649–22654.
11 A. H. de Vries, A. E. Mark and S. J. Marrink, *J. Am. Chem. Soc.*, 2004, **126**, 4488–4489.
12 S. J. Marrink and A. E. Mark, *J. Am. Chem. Soc.*, 2003, **125**, 11144–11145.
13 V. Knecht and S. J. Marrink, *Biophys. J.*, 2007, **92**, 4254–4261.
14 A. F. Smeijers, A. J. Markvoort, K. Pieterse and P. A. Hilbers, *J. Phys. Chem. B*, 2006, **110**, 13212–13219.
15 P. M. Kasson, N. W. Kelley, N. Singhal, M. Vrljic, A. T. Brunger and V. S. Pande, *Proc. Natl. Acad. Sci. U. S. A.*, 2006, **103**, 11916–11921.
16 M. J. Stevens, J. H. Hoh and T. B. Woolf, *Phys. Rev. Lett.*, 2003, **91**, 188102.
17 J. C. Shillcock and R. Lipowsky, *Nat. Mater.*, 2005, **4**, 225–228.

18 S. J. Marrink, A. H. de Vries and A. E. Mark, *J. Phys. Chem. B*, 2004, **108**, 750–760.
19 S. J. Marrink, H. J. Risselada, S. Yefimov, D. P. Tieleman and A. H. de Vries, *J. Phys. Chem. B*, 2007, **111**, 7812–7824.
20 S. Baoukina, L. Monticelli, H. J. Risselada, S. J. Marrink and D. P. Tieleman, *Proc. Natl. Acad. Sci. U. S. A.*, 2008, **105**, 10803–10808.
21 S. J. Marrink and A. E. Mark, *Biophys. J.*, 2004, **87**, 3894–3900.
22 S. E. Feller, Y. Zang, R. W. Pastor and B. R. Brooks, *J. Chem. Phys.*, 1995, **103**, 4613–4621.
23 S. J. Marrink, A. H. de Vries, T. A. Harroun, J. Katsaras and S. R. Wassall, *J. Am. Chem. Soc.*, 2008, **130**, 10–11.
24 H. J. Risselada and S. J. Marrink, *Proc. Natl. Acad. Sci. U. S. A.*, 2008, **105**, 17367–17372.
25 H. J. Risselada, A. E. Mark and S. J. Marrink, *J. Chem. Phys. B*, 2008, **112**, 7438–7447.
26 D. Van der Spoel, E. Lindahl, B. Hess, G. Groenhof, A. E. Mark and H. J. C. Berendsen, *J. Comput. Chem.*, 2005, **26**, 1701–1718.
27 H. J. C. Berendsen, J. P. M. Postma, W. F. van Gunsteren, A. Di Nola and J. R. Haak, *J. Chem. Phys.*, 1984, **81**, 3684–3690.
28 S. J. Marrink, H. J. Risselada and A. E. Mark, *Chem. Phys. Lipids*, 2005, **135**, 223–244.
29 D. P. Tieleman and S. J. Marrink, *J. Am. Chem. Soc.*, 2006, **128**, 12462–12467.
30 A. A. Gurtovenko and I. Vattulainen, *J. Phys. Chem. B*, 2007, **111**, 13554–13559.
31 C. G. Wade, *Struct. Properties Cell Membrane*, 1985, **1**, 51–76.
32 L. S. Lepore, J. F. Ellena and D. S. Cafiso, *Biophys. J.*, 1992, **61**(3), 767–775.
33 S. Leekumjorn and A. K. Sum, *Biophys. J.*, 2006, **90**, 3951–3965.
34 A. H. de Vries, A. E. Mark and S. J. Marrink, *J. Phys. Chem. B*, 2004, **108**, 2454–2463.
35 S. E. Feller, K. Gawrisch and A. D. MacKerell, Jr, *J. Am. Chem. Soc.*, 2002, **124**, 318–326.
36 A. Grossfield, S. E. Feller and P. C. Pitman, *Proc. Natl. Acad. Sci. U. S. A.*, 2006, **103**, 4888–4893.
37 M. Mihailescu and K. Gawrisch, *Biophys. J.*, 2006, **90**, L04–6.
38 A. Filippov, G. Oradd and G. Lindblom, *Biophys. J.*, 2007, **93**, 3182–3190.
39 S. P. Soni, D. S. LoCascio, Y. Liu, J. A. Williams, R. Bittman, W. Stillwell and S. R. Wassall, *Biophys. J.*, 2008, **95**, 203–214.
40 W. E. Teague, N. L. Fuller, R. P. Rand and K. Gawrisch, *Cell Mol. Biol. Lett.*, 2002, **7**, 262–264.
41 W. Stillwell and S. R. Wassall, *Chem. Phys. Lipids*, 2003, **126**, 1–27.